

## Research Article

# Adsorption and Desorption of Decane Using Non-Carbon Adsorbents

Jeongmin Park, Sang-Sup Lee\*

Department of Environmental Engineering, Chungbuk National University, Chungbuk 28644, Republic of Korea

**\*Corresponding author.**

Tel: +82-43-261-2468

E-mail: [slee@chungbuk.ac.kr](mailto:slee@chungbuk.ac.kr)

Received: 1 March 2021

Revised: 11 April 2021

Accepted: 11 May 2021

**ABSTRACT** A high concentration of volatile organic compounds (VOCs) is emitted during dry cleaning processes. Although carbonaceous materials have been widely tested for the control of VOC emission, there is a risk of fire when a large amount of VOCs is contained. Non-carbon adsorbents such as KIT-6, SBA-15, MCM-41, X-type zeolites, Y-type zeolites, aluminum silicate, and activated alumina are therefore tested in this study for the adsorption and desorption of decane which is a main constituent of VOCs emitted during dry cleaning. The adsorbents were evaluated under two conditions with and without the injection of water vapor (20% rh) using a fixed-bed reactor system. Without the injection of water vapor, KIT-6 showed the highest decane adsorption capacity, and activated alumina showed the highest decane desorption efficiency. It was also found that the mesopore volume of the adsorbent was related to its decane adsorption capacity, whereas its peak pore diameter was closely related to its decane desorption efficiency. KIT-6 showed very similar decane adsorption and desorption performance in both cases with and without the injection of water vapor. However, the decane desorption efficiency of activated alumina significantly decreased with the injection of water vapor.

**KEY WORDS** Adsorption, Desorption, Decane, Adsorbent, Non-carbon

## 1. INTRODUCTION

Volatile organic compounds (VOCs) are emitted from various sources such as dry cleaning processes, gas stations, and printing shops (Sanchez *et al.*, 2019; Wang *et al.*, 2018). The total VOC emission in South Korea in 2016 was reported to be 1,024,029 tons (Choi *et al.*, 2020; NIER, 2018). Compared to other VOC sources, the dry cleaning process can directly expose people to high concentrations of VOCs (Lee *et al.*, 2019; Viegas *et al.*, 2011; Lee *et al.*, 2009; Jo *et al.*, 2001; Räisänen *et al.*, 2001). A petroleum-based solvent is mostly used in Korean dry cleaning facilities. The petroleum-based solvent includes more than 96% C8–C12 compounds. Among them, C10 compounds are highest. As a result, the concentration of decane is highest in VOCs emitted from Korean dry cleaning facilities (Jeong *et al.*, 2003). In addition, decane has relatively high photochemical ozone creation potentials among VOCs emitted from dry cleaning facilities (Lee, 2020). Therefore, an appropriate decane control technique method is required.

Various methods have been suggested to control VOC emission, such as adsorption, absorption, condensation, biological treatment, and thermal oxidation (Khan *et al.*, 2000). Adsorption is one of the most effective and economical methods to control VOC emission (Huang *et al.*, 2018; Swetha *et al.*, 2017). Carbonaceous materials are widely used as adsorbents for VOC adsorption. Various carbonaceous materials such as activated carbon, biochar, activated carbon fiber, carbon nanotube, graphene, and carbon-silica composite have been studied and suggested as materials for controlling VOC emission (Zhang *et al.*, 2017). However, the use of carbonaceous materials is associated with a fire risk when they contain a large amount of VOCs. Non-carbon adsorbents have therefore been proposed and studied as materials for controlling VOC emission (Jeon *et al.*, 2017; Shah *et al.*, 2014; Choi *et al.*, 2013; Hu *et al.*, 2009). Mesoporous silica materials such as MCM-41, SBA-15, and KIT-6 are promising non-carbon adsorbents. MCM-41 (Mobil Composition of Matter No. 41) is a typical mesoporous material with a pore diameter of 2.38 nm and regular channels. SBA-15 (Santa Barbara Amorphous-15) and KIT-6 (Korea Institute of Technology-6) are adsorbents with a bimodal system with one-dimensional mesopore channels connected by complementary micropores. Zhang *et al.* tested MCM-41, SBA-15, SiO<sub>2</sub>, and NaY for the adsorption of toluene (Zhang *et al.*, 2012). Although NaY showed the highest adsorption capacity of 0.25 g/g for toluene, it required a high temperature for regeneration (> 350°C). SBA-15 showed the second highest adsorption capacity for toluene and required a lower desorption temperature than NaY. Dou *et al.* investigated the effect of water vapor on the adsorption of benzene onto SBA-15, MCM-41, MCM-48, and KIT-6 (Dou *et al.*, 2011), and found that KIT-6 demonstrated the best adsorption performance.

The adsorption capacities of the adsorbents decreased by 52%–54% when water vapor was injected with benzene. The decreased adsorption capacity was attributed to the fact that the silanol group (Si-OH) of the mesoporous silica became less hydrophobic in the presence of water vapor. Besides mesoporous silica, X-type and Y-type zeolite adsorbents were examined and suggested as effective adsorbents for controlling VOC emission (Kim *et al.*, 2012; Kosuge *et al.*, 2006; Brosillon *et al.*, 2001).

This study aims to find an effective non-carbon adsorbent for controlling decane emission. Despite the fact that decane is included in petroleum-based solvents and is a main constituent of VOCs emitted from the dry cleaning process (Kim *et al.*, 2017; Korea Ministry of Environment, 2002), very few studies have been conducted to investigate adsorbents for controlling decane emission. In this study, seven non-carbon adsorbents were selected and examined for their adsorption capacities and desorption efficiencies for decane.

## 2. MATERIALS AND METHODS

### 2.1 Materials

Seven commercial non-carbon adsorbents were tested. KIT-6, SBA-15, and MCM-41 were selected as mesoporous silica adsorbents. Hydrophilic X-type zeolite, hydrophobic Y-type zeolite, aluminum silicate, and activated alumina were also tested. Glass bead with a diameter of 1.5 mm was used together. Each adsorbent was analyzed for its BET surface area, pore volume, and pore diameter using an analyzer (BELSORP-mini, BEL Japan, Inc., Japan). The physical properties of these adsorbents are listed in Table 1.

**Table 1.** Physical properties adsorbents.

	Adsorbent	Type	SBET (m <sup>2</sup> /g)	Mesopore volume (cm <sup>3</sup> /g)	Micropore volume (cm <sup>3</sup> /g)	Bed composition
Mesoporous silica	KIT-6	Bead	677	0.629	0.120	0.1 g + glass beads 6 g
	SBA-15	Bead	484	0.306	0.100	
	MCM-41	Bead	889	0.557	0.073	
Zeolite	X-type	Powder	4.2	0.004	0.001	0.1 g + glass beads 6 g
	Y-type	Powder	491	0.060	0.188	
Others	Aluminum silicate	Ball (4–6 mesh)	503	0.170	0.094	0.5 g + glass beads 6 g
	Activated alumina	Ball (4–6 mesh)	226	0.335	0.021	

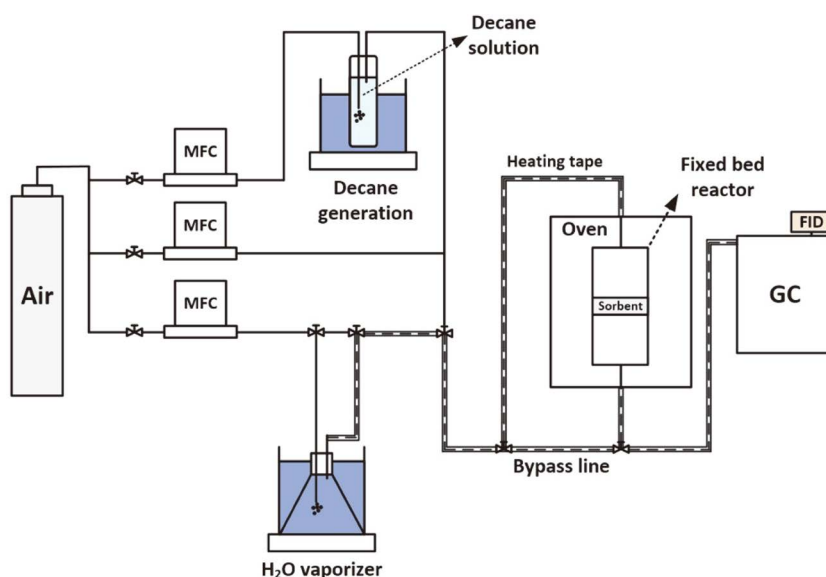


Fig. 1. Schematic of the fixed-bed reactor system for decane adsorption and desorption tests.

## 2.2 Adsorption and Desorption Test

Adsorption and desorption tests were conducted using a fixed-bed reactor system shown in Fig. 1. Each adsorbent was pre-mixed with glass beads (Model SI.5002, Daihan Scientific, Korea) and then placed inside a fixed-bed reactor at a temperature of 30°C. The height of the bed including the adsorbent and glass beads was 2 cm. From the preliminary tests of glass beads with an injection of 2,000 ppm decane, it was confirmed that glass beads have no capacity for decane adsorption. In this study, 0.1 g of KIT-6, SBA-15, MCM-41, X-type zeolite, and Y-type zeolite was used, respectively, owing to their smaller size. 0.5 g of aluminum silicate and activated alumina was used, respectively, owing to their larger size. The inlet decane concentration was 2,000 ppm considering the initial concentration of VOCs from the dry cleaning process (Korea Institute of Energy Research, 2009). Decane vapor was generated by passing 30 mL/min air through decane solution (Sigma-Aldrich, ≥ 99%) to have an inlet decane concentration of 2,000 ppm ( $\pm 15\%$ ) at a total flow rate of 150 mL/min. After a constant decane concentration was confirmed through a bypass line, 2,000 ppm ( $\pm 15\%$ ) decane was injected into the fixed-bed reactor for conducting the adsorption test. The outlet concentration of decane flowing through the fixed-bed reactor was measured by using gas chromatography (6500GC System, Youngin Chromass, Korea) with a column (YL-5, 30 m  $\times$  0.32 mm  $\times$  0.25  $\mu$ m, Youngin Chromass, Korea) and a flame ionization detector (FID). The temperatures of

Table 2. Experimental conditions.

	Adsorption	Desorption
Injection gas	2000 ppm ( $\pm 15\%$ ) decane in air with water vapor (20% rh) and without water vapor	Air
Flow rate	150 mL/min	
Temperature	30°C	
Pressure	1 atm	
Diameter of the fixed bed	1.25 cm	
Bed composition	Adsorbent with glass beads	

oven, capillary column, and FID were maintained at 150°C, 250°C, and 250°C, respectively, and the flow rate of He as carrier gas was 3 mL/min. The outlet gas was continuously flowed through the loop and sampled to the gas chromatography every 2 minutes. A calibration curve was created with five different concentrations of decane. Each decane concentration was created with a mixture of high purity air (99.999%) and decane (Sigma-Aldrich, analytical standard). Calibration was repeated 5 times at each concentration. The coefficient of determination ( $R^2$ ) for the calibration curve was determined to be 0.99.

The adsorption times for tests involving 0.1 and 0.5 g adsorbents were 60 and 180 min, respectively. Desorption test was then conducted by injecting 150 mL/min fresh

air into the fixed-bed reactor. The desorption time was the same as the adsorption time for each adsorbent. In order to investigate the effect of water vapor on each adsorbent, tests were conducted at 20% relative humidity. All adsorption and desorption tests were performed at 1 atm and 30°C. The experimental conditions are summarized in Table 2. The decane adsorption and desorption amounts were calculated from the outlet decane concentrations during each adsorption and desorption time, respectively, using the trapezoidal rule. The adsorption capacity was determined from the amount of decane adsorption per the amount of adsorbent tested. The desorption efficiency was determined from the amount of decane desorption per the amount of decane adsorption of the adsorbent.

### 3. RESULTS AND DISCUSSION

#### 3.1 Adsorption and Desorption Test Results

The seven adsorbents were first tested for decane adsorption and desorption without water vapor injection. KIT-6, SBA-15, MCM-41, X-type zeolite, and

Y-type zeolite were tested for the adsorption of decane during 60 min. Each desorption test was also conducted during 60 min. Fig. 2a shows the outlet decane concentrations during the adsorption and desorption tests of KIT-6, SBA-15, and MCM-41, respectively. Those adsorbents showed very efficient adsorption during the first 10 min. However, SBA-15 and MCM-41 became almost saturated with decane, whereas KIT-6 was not saturated with decane at the adsorption time of 60 min. In addition, KIT-6 showed higher desorption concentrations than SBA-15 and MCM-41. This indicates that KIT-6 is the most effective adsorbent among those adsorbents for controlling decane emissions. Similarly, KIT-6 showed a higher adsorption capacity for benzene than SBA-15 and MCM-41 (Dou *et al.*, 2011).

Aluminum silicate and activated alumina were tested for the adsorption and desorption of decane during 180 min. Fig. 2b shows the outlet decane concentrations during the adsorption and desorption tests of aluminum silicate and activated alumina, respectively. Aluminum silicate and activated alumina showed similar decane adsorption behavior with each other. Different from KIT-6, SBA-15, and MCM-41, aluminum silicate and

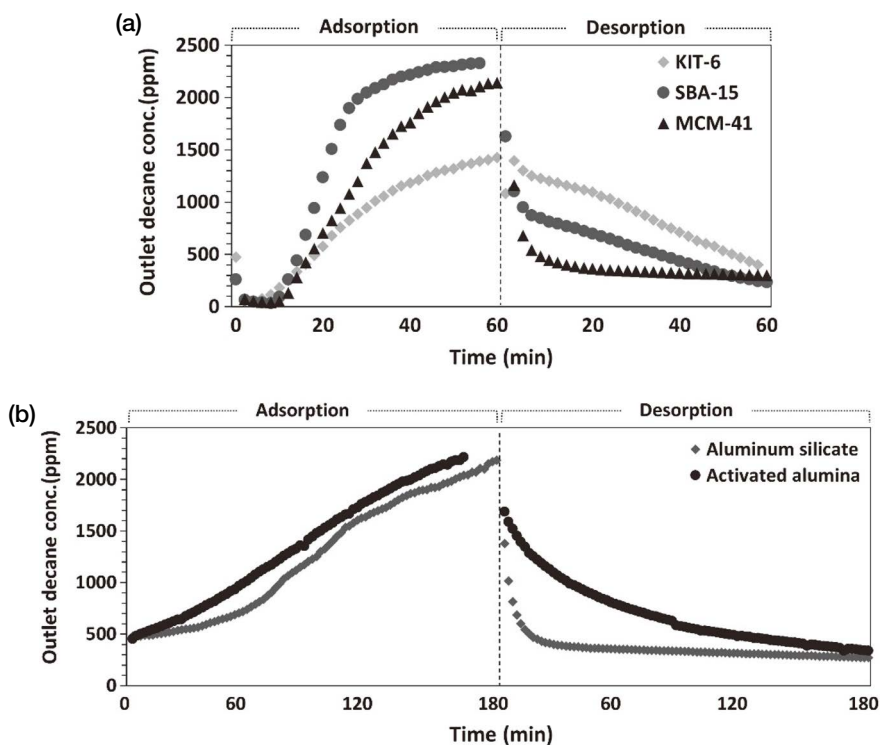


**Fig. 2.** Outlet decane concentrations with respect to the test time for (a) KIT-6, SBA-15, MCM-41, (b) aluminum silicate, and activated alumina.

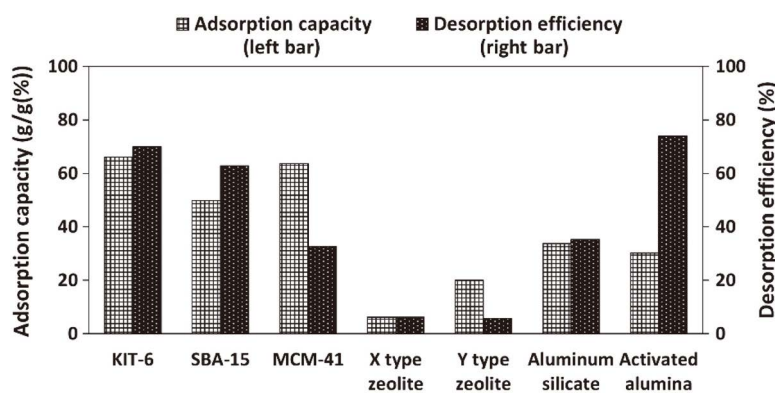


Fig. 3. Adsorption capacity and desorption efficiency of the adsorbents without the injection of water vapor.

activated alumina showed decane emissions above 400 ppm in the beginning of adsorption. This indicates that aluminum silicate and activated alumina may not be effective to adsorb decane. However, activated alumina showed a higher desorption efficiency than aluminum silicate.

The amount of decane adsorption onto each adsorbent was determined from the results shown in Fig. 2. The adsorption capacity was then determined from the amount of decane adsorption per unit amount of the adsorbent tested. The desorption efficiency was also determined from the amount of decane desorption per unit amount of decane adsorption. Fig. 3 presents the adsorption capacities and desorption efficiencies of the seven adsorbents. Because KIT-6 is not saturated with decane in the adsorption time of 60 min, Fig. 3 shows its adsorption capacity only for the adsorption time. Both X-type and Y-type zeolite adsorbents show very low decane adsorption capacities and desorption efficiencies, indicating that they are not applicable for controlling decane emissions. KIT-6, SBA-15, and MCM-41 showed high decane adsorption capacities, but MCM-41 showed low decane desorption efficiency. Although activated alumina showed a lower adsorption capacity than KIT-6, SBA-15, and MCM-41, it showed the highest desorption efficiency. Considering the low cost of activated alumina, it can be considered as an auxiliary adsorbent for controlling decane emissions.

### 3.2 Effects of Pore Volume and Diameter on Adsorption and Desorption

The mesopore volume and micropore volume of each adsorbent were determined. The adsorption capacity and the desorption efficiency are presented with respect

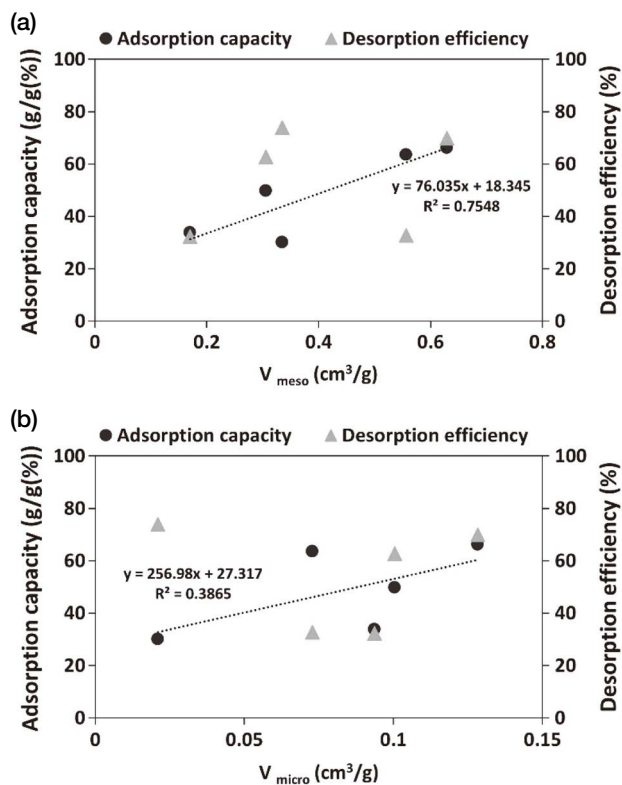


Fig. 4. Adsorption capacity and desorption efficiency with respect to (a) the mesopore volume and (b) the micropore volume of the adsorbent.

to the mesopore volume of the adsorbent, respectively, in Fig. 4a. A trend line was added for the relationship between the adsorption capacity and the mesopore volume. As shown in the figure, the adsorption capacity generally increased with an increase in the mesopore volume, whereas the desorption efficiency was not related to the mesopore volume. Fig. 4b also presents the



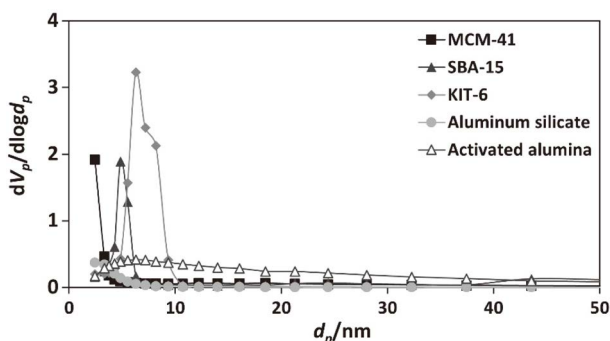


Fig. 5. Barrett-Joyner-Halenda (BJH) pore size distribution curves for the adsorbents.

adsorption capacity and the desorption efficiency with respect to the micropore volume of the adsorbent, respectively. A trend line was added for the relationship between the adsorption capacity and the micropore volume. Different from the mesopore volume, the adsorption capacity was not closely related to the micropore volume. This indicates that the mesopore volume is more responsible for the adsorption of decane than the micropore volume of the adsorbent.

Fig. 5 presents Barrett-Joyner-Halenda (BJH) pore size distribution curves for the adsorbents. MCM-41 shows the BJH pore size distribution peak at 2.44 nm whereas KIT-6 does that at 6.3 nm. Fig. 6 shows the adsorption capacity and the desorption efficiency with respect to the peak value of the BJH pore size distribution curve, respectively. As shown in the figure, the adsorption capacity was not related to the peak pore diameter. However, the desorption efficiency was closely related to the peak pore diameter with the coefficient of determination ( $R^2$ ) of 0.89. This indicates that the mesopore with a larger pore diameter is favorable for the efficient desorption of decane.

### 3.3 Effects of Water Vapor Injection on Adsorption and Desorption

KIT-6, SBA-15, MCM-41, and activated alumina, which demonstrated good performance in decane adsorption or desorption without the injection of water vapor, were further tested with the injection of water vapor. Fig. 7 shows outlet decane concentrations from the tests of KIT-6, SBA-15, MCM-41, and activated alumina with and without the injection of water vapor, respectively. As shown in the figure, KIT-6 and MCM-41 showed similar adsorption and desorption performance

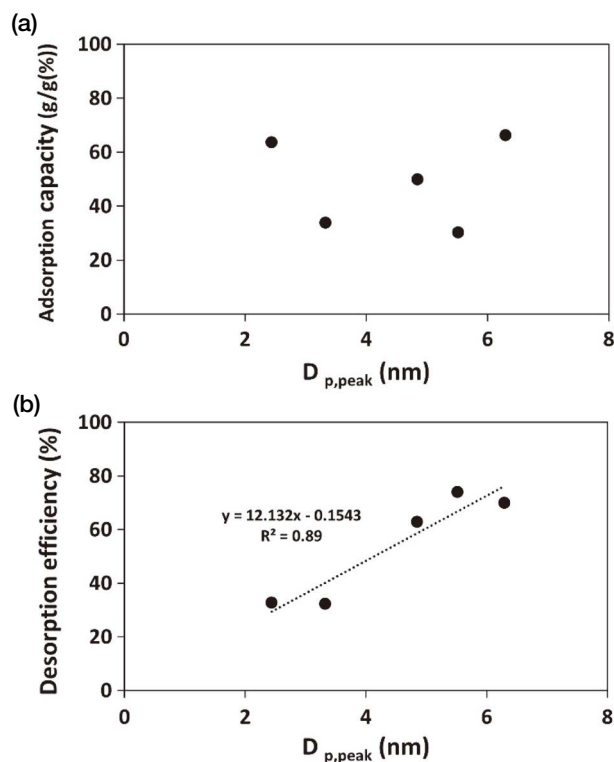
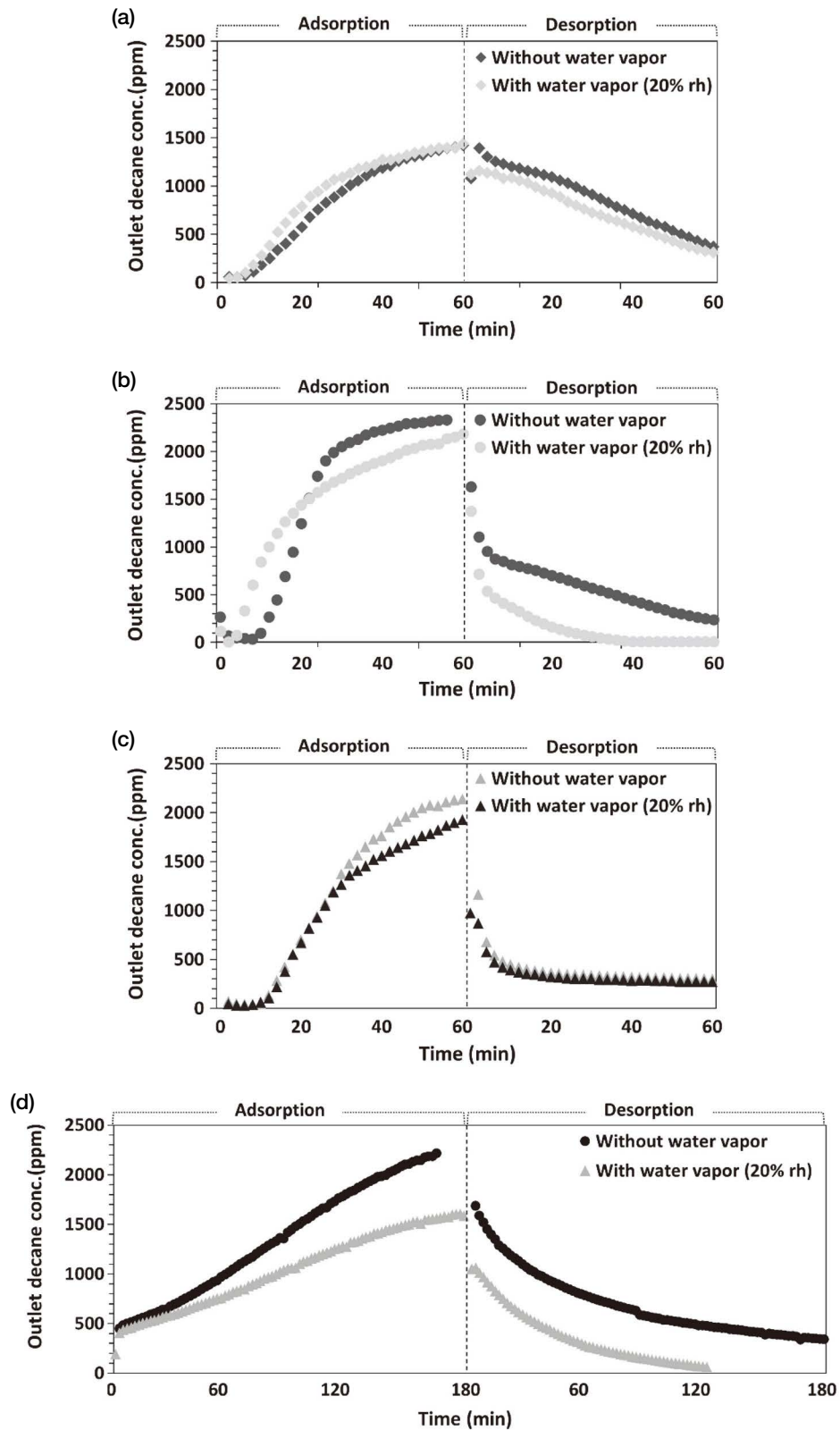


Fig. 6. Adsorption capacity (a) and desorption efficiency (b) with respect to the peak pore diameter ( $D_{p,peak}$ ) of the adsorbent.

regardless of the injection of water vapor (Fig. 7a, 7c), though those adsorbents showed significant decreases in adsorption capacities for benzene under a 13% humidity condition (Dou *et al.*, 2011). However, SBA-15 showed an earlier break point when water vapor was injected (Fig. 7b). In addition, SBA-15 showed a significant decrease in the desorption concentration of decane when water vapor was injected. Activated alumina also showed a significant decrease in the desorption concentration of decane when water vapor was injected (Fig. 7d).

Using the outlet decane concentrations shown in Fig. 7, the adsorption capacity and the desorption efficiency with the injection of water vapor (20% rh) are determined and presented in Fig. 8. With the injection of water vapor (20% rh), only KIT-6 showed the desorption efficiency of more than 60%. Comparing Fig. 3 and 8, KIT-6 and MCM-41 showed similar adsorption capacity and desorption efficiency between the cases with and without the injection of water vapor. However, SBA-15 showed a significant decrease in both adsorption capacity and desorption efficiency when water vapor was injected. Activated



**Fig. 7.** Outlet decane concentrations with respect to the test time for (a) KIT-6, (b) SBA-15, (c) MCM-41, and (d) activated alumina with and without the injection of water vapor.

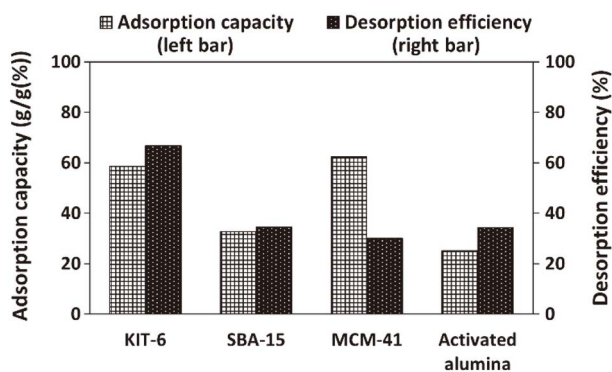


**Fig. 8.** Adsorption capacity and desorption efficiency of the adsorbents with the injection of water vapor (20% rh).

alumina showed a similar adsorption capacity but a significant decrease in desorption efficiency with the injection of water vapor. Therefore, KIT-6 also showed good performance in the adsorption and desorption of decane with the injection of water vapor, whereas SBA-15, MCM-41, and activated alumina showed low desorption efficiencies of decane. In particular, the decane desorption efficiency of activated alumina, which was the highest among the adsorbents without the injection of water vapor, significantly decreased when water vapor was injected.

#### 4. CONCLUSIONS

In order to find a non-carbon adsorbent for the adsorption of decane, seven non-carbon adsorbents were tested for the adsorption and desorption of decane. Without the injection of water vapor, mesoporous silica adsorbents showed high adsorption capacities. Judging from the adsorption capacities and desorption efficiencies of the adsorbents, KIT-6 was the most promising adsorbent for the adsorption of decane in the absence of water vapor. Activated alumina showed the highest desorption efficiency. X-type zeolite, Y-type zeolite, and aluminum silicate may not be acceptable for the adsorbents to control decane emissions. The mesopore volume of the adsorbent was found to be more closely related to its decane adsorption capacity than was the micropore volume of the adsorbent. However, the desorption efficiency was related to neither the mesopore volume nor the micropore volume of the adsorbent. The desorption efficiency was closely related to the peak pore diameter of the adsorbent with the coefficient of determination of 0.89. This suggests that the mesopore volume of the adsorbent may

be responsible for the adsorption of decane. The adsorbed decane may be more easily desorbed from the adsorbent with a higher peak pore diameter. Further tests were conducted for KIT-6, SBA-15, MCM-41, and activated alumina with the injection of water vapor (20% rh). KIT-6 and MCM-41 showed similar decane adsorption and desorption performance between the cases with and without the injection of water vapor. However, the adsorption capacity of SBA-15 and the desorption efficiency of activated alumina significantly decrease when water vapor was injected. Therefore, KIT-6 showed promising performance in the adsorption and desorption of decane in both cases with and without the injection of water vapor. In addition, activated alumina may be used as an auxiliary adsorbent for controlling decane emissions when water vapor is removed from the inlet gas.

#### ACKNOWLEDGEMENT

This research was supported by the Technology Development Program to Solve Climate Changes of the National Research Foundation (NRF) funded by the Ministry of Science, ICT (2017M1A2A2086647).

#### REFERENCES

- Azambre, B., Westermann, A., Fingueneisel, G., Can, F., Comparot, J.D. (2015) Adsorption and desorption of a model hydrocarbon mixture over HY zeolite under dry and wet conditions. *The Journal of Physical Chemistry C*, 119, 315–331. <https://doi.org/10.1021/jp509046n>
- Brosillon, S., Manero, M.H., Foussard, J.N. (2001) Mass transfer in VOC adsorption on zeolite: experimental and theoretical breakthrough curves. *Environmental Science & Technology*, 35(17), 3571–3575. <https://doi.org/10.1021/es010017x>
- Choi, J.M., Son, B.S., Kim, D.S. (2013) An Experimental Study on Explosion Hazard of Dry Cleaning Solvent Recovery Machine in Laundry. *Journal of Korean Institute of Fire Science and Engineering*, 27(1), 39–45. <https://doi.org/10.7731/KIFSE.2013.27.1.039>
- Choi, S.W., Kim, T., Lee, H.K., Kim, H.C., Han, J., Lee, K.B., Lim, E.H., Shin, S.H., Jin, H.A., Cho, E., Kim, Y.M., Yoo, C. (2020) Analysis of the National Air Pollutant Emission Inventory (CAPSS 2016) and the Major Cause of Change in Republic of Korea. *Asian Journal of Atmospheric Environment*, 14(4), 422–445. <https://doi.org/10.5572/ajae.2020.14.4.422>
- Dou, B., Hu, Q., Li, J., Qiao, S., Hao, Z. (2011) Adsorption performance of VOCs in ordered mesoporous silicas with different pore structures and surface chemistry. *Journal of Hazardous Materials*, 186, 1615–1624. <https://doi.org/10.1016/j.jhazmat.2010.12.051>



- Hu, Q., Li, J., Qiao, S., Hao, Z., Tian, H., Ma, C., He, C. (2009) Synthesis and hydrophobic adsorption properties of microporous/mesoporous hybrid materials. *Journal of Hazardous Materials*, 164, 1205–1212. <https://doi.org/10.1016/j.jhazmat.2008.09.023>
- Hu, Q., Li, J.J., Hao, Z.P., Li, L.D., Qiao, S.Z. (2009) Dynamic adsorption of volatile organic compounds on organofunctionalized SBA-15 materials. *Chemical Engineering Journal*, 149(1–3), 281–288. <https://doi.org/10.1016/j.cej.2008.11.003>
- Huang, W., Xu, J., Tang, B., Wang, H., Tan, X., Lv, A. (2018) Adsorption performance of hydrophobically modified silica gel for the vapors of n-hexane and water. *Adsorption Science & Technology*, 36, 888–903. <https://doi.org/10.1177/0263617417728835>
- Jeon, M.J., Pak, S.H., Lee, H.D., Jeon, Y.W. (2017) Practical Study of Low-temperature Vacuum Swing Adsorption Process for VOCs Removal. *Applied Chemistry for Engineering*, 28(3), 332–338. <https://doi.org/10.14478/ace.2017.1025>
- Jeong, J.Y., Yi, G.Y., Lee, N., Jeon, H.J., Kim, S.J., Kim, K.J. (2003) Characterization of petroleum-based dry cleaning solvents used in commercial dry cleaning shops for occupational exposure limit application. *Journal of Korean Society of Occupational and Environmental Hygiene*, 13(1), 74–81.
- Jo, W.K., Kim, S.H. (2001) Worker exposure to aromatic volatile organic compounds in dry cleaning stores. *American Industrial Hygiene Association*, 62(4), 466–471. <https://doi.org/10.1080/15298660108984648>
- Khan, F.I., Ghoshal, A.K. (2000) Removal of volatile organic compounds from polluted air. *Journal of Loss Prevention in the Process Industries*, 13, 527–545. [https://doi.org/10.1016/S0950-4230\(00\)00007-3](https://doi.org/10.1016/S0950-4230(00)00007-3)
- Kim, J.H., Yoo, K.S. (2017) Study on the Enhancement of VOCs Management at Laundry Facilities in Korea. *Journal of Environmental Policy and Administration Society*, 25, 139–171.
- Kim, K.J., Ahn, H.G. (2012) The effect of pore structure of zeolite on the adsorption of VOCs and their desorption properties by microwave heating. *Microporous and Mesoporous Materials*, 152, 78–83. <https://doi.org/10.1016/j.micromeso.2011.11.051>
- Korea Institute of Energy Research(KIER) (2009) Development of 3 Nm<sup>3</sup>/hr scale electric heating system for the treatment of VOCs from laundry, Korea Ministry of Environment.
- Korea Ministry of Environment (2002) A Study on the Contribution of Solvent to Air Pollution, Report, Korea, October.
- Kosuge, K., Kubo, S., Kikukawa, N., Takemori, M. (2006) Effect of pore structure in mesoporous silicas on VOC dynamic adsorption/desorption performance. *Langmuir*, 23, 3095–3102. <https://doi.org/10.1021/la062616t>
- Lee, H., Song, M., Kim, D. (2019) Estimation of Emissions and Emission Factor of Volatile Organic Compounds from Small-scale Dry Cleaning Operations Using Organic Solvents. *Journal of Korean Society for Atmospheric Environment*, 35(4), 413–422.
- Lee, H.J. (2020) Characteristics of Volatile Organic Compounds Emission from Small-scale Dry Cleaning Process and its effects on Ambient Atmospheric Environment, Seoul National University of Science And Technology, Seoul.
- Lee, S.J., Moon, S.H. (2009) Adsorption of VOCs from Dry Cleaning. *Journal of Korean Society of Environmental Engineers*, 31, 1025–1032.
- NIER (National Institute of Environmental Research) (2018) National air pollution emission, Report, Korea, July.
- Räisänen, J., Niemelä, R., Rosenberg, C. (2001) Tetrachloroethylene emissions and exposure in dry cleaning. *Journal of the Air & Waste Management Association*, 51(12), 1671–1675. <https://doi.org/10.1080/10473289.2001.10464396>
- Sanchez, N.P., Saffari, A., Barczyk, S., Coleman, B.K., Naufal, Z., Rabideau, C., Pacsi, A.P. (2019) Results of Three Years of Ambient Air Monitoring Near a Petroleum Refinery in Richmond, California, USA. *Atmosphere*, 10(7), 385. <https://doi.org/10.3390/atmos10070385>
- Shah, I.K., Pre, P., Alappat, B.J. (2014) Effect of thermal regeneration of spent activated carbon on volatile organic compound adsorption performances. *Journal of the Taiwan Institute of Chemical Engineers*, 45(4), 1733–1738. <https://doi.org/10.1016/j.jtice.2014.01.006>
- Swetha, G., Gopi, T., Shekar, S.C., Ramakrishna, C., Saini, B., Rao, P.V.L. (2017) Combination of adsorption followed by ozone oxidation with pressure swing adsorption technology for the removal of VOCs from contaminated air streams. *Chemical Engineering Research and Design*, 117, 725–732. <https://doi.org/10.1016/j.chemd.2016.11.036>
- Viegas, S. (2011) Occupational exposure to perchloroethylene in Portuguese dry-cleaning stores. *WIT Transactions on Ecology and the Environment*, 147, 247–254.
- Wang, F., Zhang, Z., Acciai, C., Zhong, Z., Huang, Z., Lonati, G. (2018) An integrated method for factor number selection of PMF model: Case study on source apportionment of ambient volatile organic compounds in Wuhan. *Atmosphere*, 9(10), 390. <https://doi.org/10.3390/atmos9100390>
- Zhang, W., Qu, Z., Li, X., Wang, Y., Ma, D., Wu, J. (2012) Comparison of dynamic adsorption/desorption characteristics of toluene on different porous materials. *Journal of Environmental Sciences*, 24, 520–528. [https://doi.org/10.1016/S1001-0742\(11\)60751-1](https://doi.org/10.1016/S1001-0742(11)60751-1)
- Zhang, X., Gao, B., Creamer, A.E., Cao, C., Li, Y. (2017) Adsorption of VOCs onto engineered carbon materials: A review. *Journal of Hazardous Materials*, 338, 102–123. <https://doi.org/10.1016/j.jhazmat.2017.05.013>